Period doubling in four-dimensional symplectic maps

Jian-Min Mao
Center for Studies of Nonlinear Dynamics, La Jolla Institute, 3252 Holiday Court, Suite 208, La Jolla, California 92037

Indubala I. Satija*
Center for Nonlinear Studies, Los Alamos National Laboratory, University of California, Los Alamos, New Mexico 87545

Bambi Hu
Department of Physics, University of Houston—University Park, Houston, Texas 77004
(Received 9 December 1985)

A complete period-doubling sequence in four-dimensional symplectic maps is determined by following a special bifurcation pass in the parameter plane. Stability diagrams for lower periods in the parameter plane are shown. Within numerical accuracy, there exist certain relations between the scaling exponents of the period-doubling sequence.

I. INTRODUCTION

The method of the Poincaré "surface of sections" is very informative in the study of dynamical systems. In a Hamiltonian system with n degrees of freedom, the Poincaré section defines a $2(n-1)$-dimensional symplectic map. Period doubling in Hamiltonian systems can then be profitably studied via these Poincaré maps.

Extensive studies of period doubling in one-dimensional (1D) maps have been made. However, period doubling in higher dimensions is relatively poorly understood. For dissipative systems described by volume-contracting maps, it has been shown that the universal behavior reduces to that of one dimension. However, for conservative systems with two degrees of freedom such as those described by two-dimensional (2D) area-preserving maps, the universal ratios have been found to be distinctly different.[1–4] Not much is known about period doubling in conservative systems for $d \geq 3$. The following question has attracted a great deal of interest in recent years.[5–9] Do maps corresponding to Hamiltonian systems with three or more degrees of freedom exhibit an infinite sequence of period-doubling bifurcations? And, if so, do they introduce new universality classes?

In this paper, we have studied period doubling in four-dimensional (4D) symplectic maps which model Hamiltonian systems with three degrees of freedom. In Sec. II, a stability analysis of period doubling in four dimensions is given. A detailed account of how a complete period-doubling sequence was located is given in Sec. III. The application of the scaling-matrix method to compute the scaling factors is described in Sec. IV. Finally, a summary is given in Sec. V.

II. STABILITY ANALYSIS

A. Eigenvalues of symplectic maps

The eigenvalues of the Jacobian matrix of a linearized symplectic map L come in pairs.[5] For a 4D symplectic map, the eigenvalues are of the form $\lambda_1, 1/\lambda_1, \lambda_2, 1/\lambda_2$, and the characteristic equation is

$$\lambda^4 - t_1\lambda^3 + t_2\lambda^2 - t_1\lambda + 1 = 0 , \tag{1}$$

where

$$t_1 = \mathrm{Tr}L = \lambda_1 + 1/\lambda_1 + \lambda_2 + 1/\lambda_2 , \tag{2a}$$

$$t_2 = \mathrm{Tr}L_{12} = 2 + (\lambda_1 + 1/\lambda_1)(\lambda_2 + 1/\lambda_2) . \tag{2b}$$

Here

$$\mathrm{Tr}L_{12} = \sum_{\substack{i,j \\ i<j}} (L_{ii}L_{jj} - L_{ij}L_{ji})$$

is the other invariant of the matrix besides $\mathrm{Tr}L$. To simplify notations, let

$$k_1 = \lambda_1 + 1/\lambda_1 , \tag{3a}$$

$$k_2 = \lambda_2 + 1/\lambda_2 . \tag{3b}$$

Then,

$$t_1 = k_1 + k_2 , \tag{4a}$$

$$t_2 = 2 + k_1 k_2 . \tag{4b}$$

The solutions of the above equations are, respectively,

$$k_{1,2} = \tfrac{1}{2}[t_1 \pm (t_1^2 - 4t_2 + 8)^{1/2}] , \tag{5}$$

$$\left.\begin{matrix}\lambda_1 \\ 1/\lambda_1\end{matrix}\right\} = \tfrac{1}{2}[k_1 \pm (k_1^2 - 4)] . \tag{6}$$

$$\left.\begin{matrix}\lambda_2 \\ 1/\lambda_2\end{matrix}\right\} = \tfrac{1}{2}[k_2 \pm (k_2^2 - 4)] . \tag{7}$$

B. Stability regions

The stability of a fixed point at which linearization is performed is determined by the eigenvalues of the Jacobian matrix. From Eqs. (5)–(7), the eigenvalues depend on three discriminants. Zero discriminants are given when one of the following conditions is satisfied:

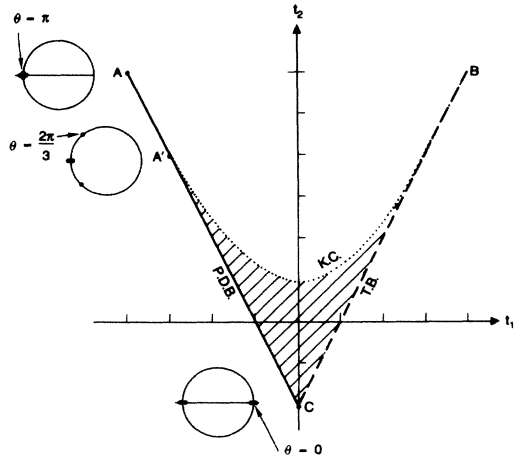

FIG. 1. Stable region for 4D symplectic maps. The shaded region is stable. The period-doubling bifurcation line, tangent bifurcation line, and Krein crunch curve are represented, respectively, by solid, dashed, and dotted curves.

$$t_2=\tfrac{1}{4}t_1^2+2\ , \tag{8}$$

$$t_2=\pm 2t_1-2\ . \tag{9}$$

These three curves bound a stable region, the shaded region in Fig. 1. Period-doubling bifurcations occur when the corresponding points in the plane pass the period-doubling bifurcations line segment AC. The line BC is the tangent bifurcation line, and the parabola BC is the Krein crunch curve. The three vertices will be called the A, B, and C point.

III. COMPLETE PERIOD-DOUBLING SEQUENCE

A. Bifurcation point

Let us first review the bifurcation conditions for one- and two-dimensional maps. In 1D dissipative maps $x_{i+1}=f_a(x_i)$, the bifurcation from period-2^n to period-2^{n+1} occurs when the linearized map L, a 1×1 matrix, is -1. That is,

$$\mathrm{Tr}L=-1 \tag{10}$$

is the bifurcation point on the TrL axis, as shown in Fig. 2.

In 2D area-preserving maps, TrL is the only changeable invariant of the linearized map L because the other invariant $\det L\equiv 1$. Bifurcation occurs when the eigenvalues λ and $1/\lambda$ reach -1, which requires $\mathrm{Tr}L=-2$. The bifurcation point on the TrL axis is also a point, as shown in Fig. 3.

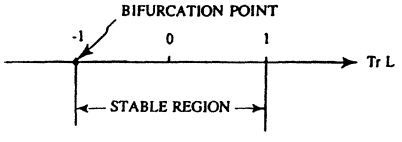

FIG. 2. Bifurcation point for 1D maps.

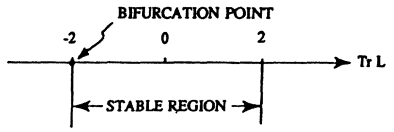

FIG. 3. Bifurcation point for 2D area-preserving maps.

Now we turn to 4D symplectic maps. As shown in Fig. 1, a period-doubling bifurcation occurs when one crosses the line segment AC, where a pair of eigenvalues (say, λ_1 and $1/\lambda_1$) reach -1. There is an infinite number of possible bifurcation points: All points on the line segment could be bifurcation points.

Period doubling produces a pattern that promises the property of self-similarity, i.e., the pattern generated by applying the map 2^n times contains parts which are similar to one another and also to the pattern generated by applying the map 2^{n-1} times. This self-similarity requires that the eigenvalues of the linearized map L (and its invariants, t_1 and t_2) for the nth bifurcation should be the same as that for all the orders of period-doubling bifurcations. One should then study all orders of period-doubling bifurcations at the same bifurcation point in the t_1t_2-plane. For instance, if one chooses a point on the line AC as a bifurcation point for the nth period-doubling bifurcation, then one should use the same point as the bifurcation point for all higher orders of period-doubling bifurcations.

Any point on the period-doubling bifurcation line AC (Fig. 1) could be the bifurcation point. The bifurcation point corresponds to an eigenvalue configuration $(\lambda_1,1/\lambda_1,\lambda_2,1/\lambda_2)=(-1,-1,e^{i\theta},e^{-i\theta})$. There are three special values of θ, $\theta=0,2\pi/3,\pi$. For the first two θ's the second pair of eigenvalues interchange when the period doubles. In this sense they give the "best" self-similarity. For $\theta=\pi$, bifurcation occurs when $(\lambda_1,1/\lambda_1)=(-1,-1)$ and $(\lambda_2,1/\lambda_2)=(-1,-1)$. It is the same as how the two independent 2D area-preserving maps behave.

In this paper we choose the C point ($\theta=0$, Fig. 1) as the bifurcation point; that is,

$$(t_1,t_2)=(0,-2)\ , \tag{11}$$

corresponding to the eigenvalues $-1,-1,1,1$. These eigenvalues become $+1,+1,+1,+1$ when the period doubles, see Fig. 4.

B. Two-parameter search

Most of the 1D dissipative maps and 2D area-preserving maps studied previously belong to one-parameter family of maps. However, for 4D symplectic maps, we have to introduce two parameters to locate a complete period-doubling sequence. The rationale is as follows.

Consider a 4D symplectic map

$$T_a:\ \mathbf{x}\rightarrow T_a\mathbf{x}\ , \tag{12}$$

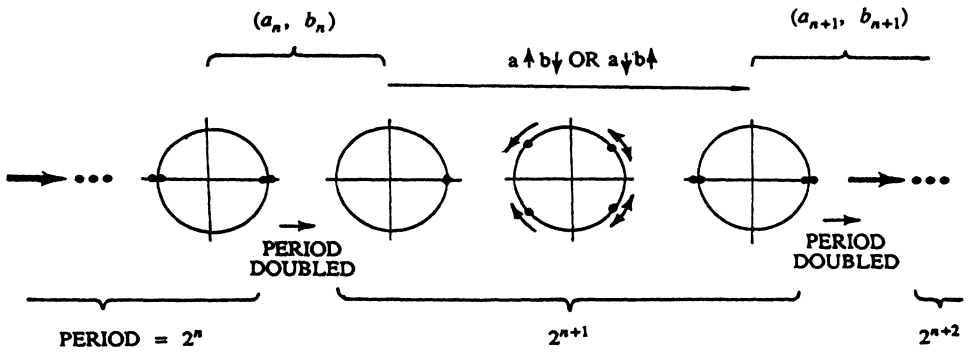

FIG. 4. Eigenvalue behavior for the 4D symplectic map. The a and b are parameters of the map.

where $\mathbf{a}$ is a parameter vector whose dimension d is yet unknown, and $\mathbf{x}$ is a 4-vector. Let $\mathbf{x}_0^{(n)}$ denote a fixed point of period 2^n, i.e.,

$$\mathbf{x}_0^{(n)} = T_{\mathbf{a}}^{(2^n)} \mathbf{x}_0^{(n)} . \tag{13}$$

From previous discussions, the nth-order bifurcation occurs when Eq. (11) is satisfied, where t_1 and t_2 are functions of $\mathbf{a}$ and $\mathbf{x}_0^{(n)}$.

Now we have six equations [four in Eq. (13) and two in Eq. (11)] for $(4+d)$ unknowns (four for $\mathbf{x}_0^{(n)}$ and d for $\mathbf{a}$). It is obvious that one has to choose $d=2$, i.e., one has to consider a two-parameter family of 4D symplectic maps to search for a complete period-doubling sequence.

C. Hénon-like 4D symplectic map

Now we start to study the period-doubling bifurcation behavior for a Hénon-like 4D symplectic map:

$$T: \begin{cases} X' = -Y + F_{a,b}(X) , \\ Y' = X , \end{cases} \tag{14}$$

where X and Y are 2-vectors,

$$X = \begin{bmatrix} x \\ z \end{bmatrix} , \quad Y = \begin{bmatrix} y \\ t \end{bmatrix} , \tag{15}$$

and $F_{a,b}$ is a nonlinear transformation,

$$X \to F_{a,b}(X) = \begin{bmatrix} f_{a,b}(x,z) \\ g_{a,b}(x,z) \end{bmatrix} . \tag{16}$$

where a and b are parameters.

The map (14), in vector-matrix form, can be written explicitly,

$$T: \begin{cases} x' = -y + f_{a,b}(x,z) , \\ z' = -t + g_{a,b}(x,z) , \\ y' = x , \\ t' = z . \end{cases} \tag{17}$$

If $f_{a,b}(x,z)$ is a function of x, and $g_{a,b}(x,z)$ a function of z only, then one comes back to the 2D Hénon map.

It is easy to check that the map (17) is symplectic if and only if

$$\frac{\partial f_{a,b}}{\partial z} = \frac{\partial g_{a,b}}{\partial x} . \tag{18}$$

To make the map symplectic, one can choose

$$\begin{aligned} f_{a,b}(x,z) &= 1 - a h(x) - b(x+z) , \\ g_{a,b}(x,z) &= 1 - a h(z) - b(x-z) , \end{aligned} \tag{19}$$

where $h(x) = x^2$ is nonlinear.

One may generalize the discussion[10] about the factorization into involutions, the dominant symmetry curves of the 2D Hénon map to that of the 4D Hénon-like symplectic map. The map (14), or its equivalent (17), can be factorized as a product of two involutions I_1 and I_2,

$$T = I_2 I_1 , \tag{20}$$

$$I_1: \begin{cases} X' = Y \\ Y' = X , \end{cases} \tag{21}$$

$$I_2: \begin{cases} X' = -X + F(Y) \\ Y' = Y . \end{cases} \tag{22}$$

There are two symmetry surfaces:

$$2Y = F_{a,b}(X) \tag{23}$$

and

$$Y = X . \tag{24}$$

D. Stable regions in parameter plane

To exhibit more a explicit picture of period doubling, we transform the stability diagrams from the trace plane ($t_1 t_2$ plane, Fig. 1) to the parameter plane (ab plane, Fig. 5).

The period-1 stable regions in the parameter plane are labeled by 1_1 and 1_2 in Fig. 5. They have a common Krein crunch line $b=0$. The point ${}^1A_1$ $[(a,b)=(3,0)]$ is the period-1 image of the A point $[(t_1,t_2)=(-4,6)]$. (Images of the A point are labeled by ${}^N A_1$ in Fig. 5, where N is the period, and $i=1,2,\ldots$. Images of the C point are labeled by ${}^N C_i$). The point ${}^1C_1$ $[(a,b)=(-1,2)]$ is the

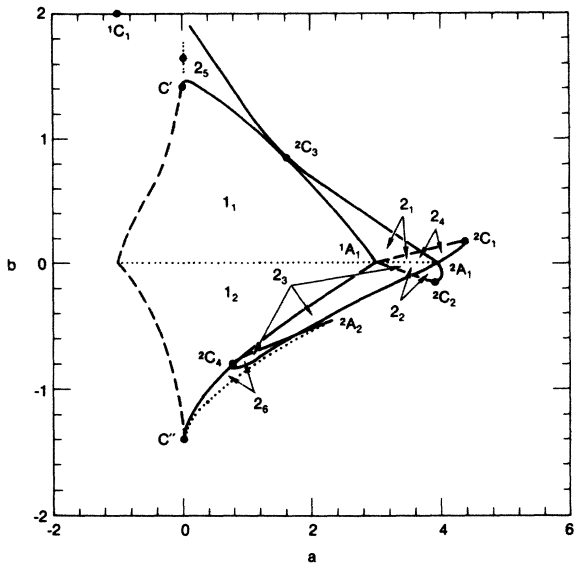

FIG. 5. Stable regions for periods 1 and 2 in the parameter plane. Stable regions are labeled by N_i, where N is the period and $i=1, 2, \ldots$. The images of the A and the C points are labeled by ${}^N A_i$ and ${}^N C_i$, respectively. The period-doubling bifurcation curves, tangent bifurcation curves, and the Krein crunch curves are, respectively, represented by solid, dashed, and dotted curves.

period-1 image of the C point. But the points $(a,b)=(0,\pm\sqrt{2})$ are not in the period-1 stable region since the coordinates of the period-1 orbits tend to infinites when $(a,b)\rightarrow(0,\pm\sqrt{2})$.

The period-2 stable regions are labeled by 2_i, $i=1, 2, \ldots, 6$ in Fig. 5. Some of them overlap. As an example of how we locate the stable regions, the period-doubling bifurcation curve ${}^2C_3\,{}^2A_1$ is determined by gradually varying the parameter from point ${}^2C_3$ while choosing such a periodic orbit that the orbit varies gradually also. Figure 5 shows that the stable regions 2_1 and 2_2 are born when passing the period-doubling bifurcation curve ${}^2C_3\,{}^1A_1$, the regions 2_3 and 2_4 are born when passing through the period-doubling bifurcation curve ${}^2C_4\,{}^1A_1$, region 2_5 through the curve ${}^2C_3C'$, and region 2_6 through the curve ${}^2C_4C''$.

The correspondence of the stable regions to the period-doubling bifurcation curves restricts where the successive bifurcation can occur: if the first-order bifurcation occurs at a point on the period-doubling bifurcation curve ${}^2C_3\,{}^1A_1$, for instance, then the second-order bifurcation would occur at a point on either curve ${}^2C_3\,{}^2A_1$ or ${}^2C_2\,{}^2A_1$. It is also because we are interested only in the self-similar period doubling.

Period-4 (or higher) stable regions are much more complicated. The stable regions for successively higher periods should have a similar pattern as those for lower periods.

E. Bifurcation pass

Consider the C point as the bifurcation point. It becomes the B point (see Fig. 1) when the period doubles. We may vary the parameters in such a way that t_1 and t_2 vary along the tangent bifurcation curve onto the C point. (This is a reasonable, though not unique way.) When we reach the C point the period doubles again, and so on. A pass will be finally formed in the parameter plane. We call this special bifurcation pass the C pass.

There are a huge number of C passes. Since the stable regions for higher periods are very complex, not every C pass will give rise to a complete period-doubling sequence in general. A successful C pass, which does give rise to a complete period-doubling sequence, will be described in the next subsection.

F. A complete period-doubling sequence

As seen from Fig. 5 the period-1 image of the C point, ${}^1C_1$, is isolated from the stable region. Hence, the first period-doubling bifurcation could not occur at the point

TABLE I. Convergence of the critical values of the parameters a and b for the four-dimensional Hénon-like symplectic map (17) with the nonlinear term $h(x)=x^2$.

Period 2^n n	a	b
2	3.154 929 859 908 943	0.286 068 854 598 499 3
3	3.310 106 308 833 480	0.244 813 629 780 800 7
4	3.302 711 501 079 377	0.249 186 673 247 677 3
5	3.303 272 425 207 033	0.249 158 055 154 258 2
6	3.303 252 894 478 887	0.249 185 866 130 813 6
7	3.303 256 133 362 466	0.249 187 022 559 878 9
8	3.303 256 140 697 924	0.249 187 290 167 154 2
9	3.303 256 165 659 491	0.249 187 311 907 233 6
10	3.303 256 166 921 683	0.249 187 315 307 924 1
11	3.303 256 167 172 515	0.249 187 315 307 924 1
12	3.303 256 167 194 240	0.249 187 315 346 598 6
13	3.303 256 167 197 198	0.249 187 315 350 860 1
14	3.303 256 167 197 506	0.249 187 315 351 360 3
15	3.303 256 167 197 543	0.249 187 315 351 416 8
16	3.303 256 167 197 548	0.249 187 315 351 423 4

TABLE II. Convergence of the orbital elements in the period-doubling sequence for the four-dimensional Hénon-like symplectic map (17) with the nonlinear term $h(x)=x^2$.

Period 2^n n	x_0	z_0
2	−0.013 348 468 196	0.109 592 718 271
3	0.045 304 934 297	0.077 726 692 247
4	0.034 817 130 742	0.084 811 195 923
5	0.037 620 505 763	0.083 700 731 234
6	0.036 954 792 969	0.083 984 618 545
7	0.037 124 448 841	0.083 918 315 010
8	0.037 082 664 342	0.083 935 119 540
9	0.037 093 115 639	0.083 930 986 927
10	0.037 090 520 432	0.083 932 020 270
11	0.037 091 166 996	0.083 931 763 716
12	0.037 091 006 159	0.083 931 827 633
13	0.037 091 046 197	0.083 931 811 734
14	0.037 091 036 233	0.083 931 815 692
15	0.037 091 038 713	0.083 931 814 707
16	0.037 091 038 096	0.083 931 814 952

$^1C_1$. However, since we are interested only in the asymptotic behavior of period-doubling, asymptotic self-similar period doubling can start at any period.

In order to follow the C pass described in the last subsection we first locate the period-4 image of the C point at

$$(a,b)=(3.154,0.2864)\ . \tag{25}$$

Then, doubling the period and following the period-8 image of the tangent bifurcations line BC, we reach the period-8 image of the C point,

$$(a,b)=(3.310,0.2448)\ , \tag{26}$$

and so on.

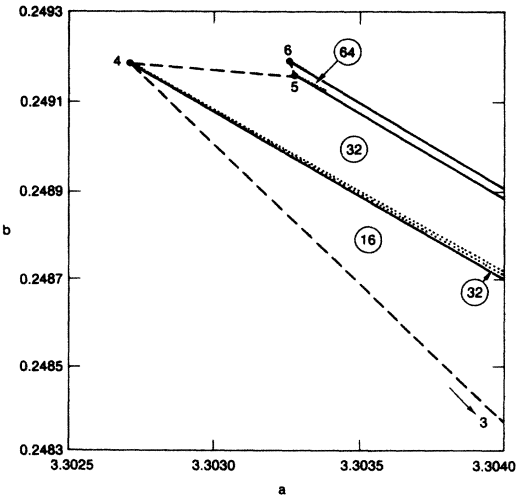

FIG. 6. Stability in the neighborhood of the C pass. Circled numbers indicate periods. Note that there are two period-32 stable regions indicated by circled 32's. The dots denote period-doubling bifurcation points, and the number beside them indicates the order of bifurcation.

Continuing to search for higher orders of bifurcation in the same way, we have succeeded in finding a period-doubling bifurcation sequence up to period 2^{16}. We believe that bifurcations can be found even for periods higher than 2^{16}. In this sense, the period-doubling sequence we found in the 4D map is an infinite one. The bifurcation values of parameters are listed in Table I. The bifurcation values of orbital elements are listed in Table II.

The stability in the neighborhood of the C pass followed is shown in Fig. 6 for periods 16, 32, and 64. There are two period-32 stable regions marked as circled 32's between which we have Krein crunch. The period-16 stable region is connected to the upper period-32 region only at one point, the point marked as 4 (the period-16 image of the C point). This is typical for all higher periods: The stable regions for successive periods in the neighborhood of the C pass are connected only at one point, the C point.

IV. SCALING FACTORS

Consider a period-doubling bifurcation sequence for one (a, say) of the parameters and let $\{a_n\}=\{a_0, a_1, a_2, \dots\}$, where a_n is the critical value of parameter a at which the $(n+1)$th period-doubling bifurcation from period 2^n to 2^{n+1} occurs.

One then tests whether or not the sequence $\{a_n\}$ converges geometrically with a rate

$$\delta=\lim_{n\to\infty}\delta_n\ ,\qquad \delta_n=(a_{n-1}-a_{n-2})/(a_n-a_{n-1})\ . \tag{27}$$

If it does, then one says the sequence has a scaling behavior.

For one of the two parameters in 4D symplectic maps, δ_n as determined by Eq. (27) converges very slowly to a value between 8 and 9. It nevertheless encourages us to look for a "better" scaling if any.

A. Scaling-matrix method

Guckenheimer, Hu, and Rudnick[11] developed a general method of testing for scaling. To introduce this method, consider two scalar sequences $\{u_n\}$ and $\{v_n\}$, whose scalings are to be tested. Instead of testing for scaling of the two sequences separately, they suggest to test a vector sequence $\{\nu_n\}=\{(u_n,v_n)\}$. They then define a scaling matrix $\tilde{C}_n$ by

$$\nu_{n-1}=\tilde{C}_n\nu_n \tag{28}$$

and then test whether or not $\tilde{C}_n$ converges to a constant matrix $\tilde{C}$. If it does, then one can say that the two scalar sequences together have scaling behavior.

B. Scaling matrix of parameters

Using this scaling-matrix method, we consider the two parameters a and b in the 4D maps as components of a vector, and then construct a parameter-difference vector sequence

$$\{\nu_n\}=\{(\Delta a_n,\Delta b_n)\}\ , \tag{29}$$

where $\Delta a_n=a_n-a_{n-1}$, $\Delta b_n=b_n-b_{n-1}$. It is suggested that

$$\nu_{n-1}=\tilde{\delta}_n\nu_n\ , \tag{30}$$

where $\tilde{\delta}_n$ is a 2×2 matrix, or explicitly,

$$\begin{bmatrix}\Delta a_{n-1}\\ \Delta b_{n-1}\end{bmatrix}=\begin{bmatrix}\delta_{11}^{(n)} & \delta_{12}^{(n)}\\ \delta_{21}^{(n)} & \delta_{22}^{(n)}\end{bmatrix}\begin{bmatrix}\Delta a_n\\ \Delta b_n\end{bmatrix}\ . \tag{31}$$

A numerical calculation using the data of the critical values of the parameters in Table I shows that the scaling matrix converges very fast,

$$\tilde{\delta}_n\to\tilde{\delta}=\begin{bmatrix}\delta_{11} & \delta_{12}\\ \delta_{21} & \delta_{22}\end{bmatrix}=\begin{bmatrix}-10.49 & 7.126\\ 12.37 & 4.128\end{bmatrix}\ \text{as}\ n\to\infty\ . \tag{32}$$

The good convergence indicates the existence of scaling for the vector sequence.

C. Invariants of the scaling matrix

Independent invariants of the 2×2 matrix $\tilde{\delta}$ are its determinant and trace (or its two eigenvalues). The diagonalized matrix of the nth scaling matrix $\tilde{\delta}_n$ is of the form

$$\begin{bmatrix}\delta_{1n} & 0\\ 0 & \delta_{2n}\end{bmatrix}\to\begin{bmatrix}\delta_1 & 0\\ 0 & \delta_2\end{bmatrix}\ \text{as}\ n\to\infty\ , \tag{33}$$

where δ_{1n} and δ_{2n} are the eigenvalues of the nth scaling matrix. It is found that the limit of one eigenvalue is just the parameter convergence rate for 2D area-preserving maps (see Table III),

$$\delta_{1n}\to\delta_1=8.721\,097\,2\ \text{ as}\ n\to\infty \tag{34a}$$

and the limit of the other eigenvalue is

$$\delta_{2n}\to\delta_2=-15.0786\ \text{ as}\ n\to\infty\ . \tag{34b}$$

The existence of two convergence rates for the parameter implies that, in the renormalization-group scheme, the fixed-point function has two relevant unstable directions under the period-doubling operator with the eigenvalues δ_1 and δ_2. From Eq. (30), one can easily obtain

$$\begin{aligned}\nu_n&=(\mathrm{Tr}\tilde{\delta}_n)\nu_{n+1}-(\det\tilde{\delta}_n)\nu_{n+2}\\ &=(\delta_{1n}+\delta_{2n})\nu_{n+1}-(\delta_{1n}\delta_{2n})\nu_{n+2}\ .\end{aligned} \tag{35}$$

That is, the element of the vector sequence depends not only on the previous element, but also on the one before that.

The values of δ_1 and δ_2 in Eqs. (34a) and (34b) satisfy $\delta_2=2\alpha_1\beta_1/\delta_1$ within the numerical accuracy, where $\alpha_1=-4.018\,076$ and $\beta_1=16.3638$ are the orbital scaling factors in 2D area-preserving maps. We have no clue as to why there exists such relations.

D. Two relevant directions

The two parameter convergence rates in Eqs. (34a) and (34b) are those along the two relevant directions (the Feigenbaum critical lines) in the parameter plane. Let these two lines be in the form, for n large,

TABLE III. Period-doubling bifurcation rates δ_1 and δ_2, and orbital scaling factors α_1 and α_2, β_1, and β_2 along and across the dominant symmetry surface, respectively, for the four-dimensional Hénon-like symplectic map (17) with the nonlinear term $h(x)=x^2$.

Period 2^n n	δ_1	δ_2	α_1	α_2	β_1	β_2
5	9.394 969 0	−17.738 353	−4.727 903 416	−19.326 037	6.206 889	6.206 889 8
6	8.847 625 6	−16.842 358	−4.030 998 823	16.965 790	13.169 810	13.169 810 9
7	8.723 543 0	−15.303 906	−4.017 347 408	15.955 490	15.579 237	−8.743 703 7
8	8.722 287 7	−15.049 664	−4.018 263 781	16.183 370	15.876 244	−7.693 843 1
9	8.721 100 0	−15.092 972	−4.018 066 838	16.135 221	16.214 081	−7.539 500 3
10	8.721 109 7	−15.075 200	−4.018 079 299	16.148 114	16.261 098	−7.545 727
11	8.721 096 6	−15.079 738	−4.018 076 571	16.143 809	16.314 274	−7.538 013 1
12	8.721 097 2	−15.078 419	−4.018 076 740	16.145 397	16.335 769	−7.539 838 0
13	8.721 097 2	−15.078 773	−4.018 076 703	16.144 747	16.349 052	−7.539 211 2
14	8.721 097 2	−15.078 672	−4.018 076 705	16.145 025	16.355 799	−7.539 390 0
15	8.721 097 2	−15.078 641	−4.018 076 704	16.144 902	16.359 544	−7.539 336 8
16	8.721 097 2	−15.078 659	−4.018 076 704	16.144 957	16.361 541	−7.539 352 0

$$a_n = r b_n + c \ , \tag{36}$$

then

$$\Delta a_n = r \Delta b_n \ . \tag{37}$$

From (31) we know that, for n large,

$$\Delta a_n = \delta_{11} \Delta a_{n+1} + \delta_{12} \Delta b_{n+1} \ , \tag{38a}$$

$$\Delta b_n = \delta_{21} \Delta a_{n+1} \delta_{22} \Delta b_{n+1} \ . \tag{38b}$$

By Eq. (37) they can be written as

$$\Delta a_n = (\delta_{11} + \delta_{12}/r) \Delta a_{n+1} \ , \tag{39a}$$

$$\Delta b_n = (\delta_{21} r + \delta_{22}) \Delta b_{n+1} \ . \tag{39b}$$

The quotient of these two equations gives

$$\delta_{21} r^2 + (\delta_{22} - \delta_{11}) r - \delta_{12} = 0 \ . \tag{40}$$

Its solutions are

$$r_{1,2} = \frac{1}{2\delta_{21}} \{ \delta_{11} - \delta_{22} \pm [(\delta_{22} - \delta_{11})^2]^2 + 4\delta_{12}\delta_{21} \} \ . \tag{41}$$

Using the data for δ_{ij}'s given in Eq. (32), we have

$$r_{1,2} = \begin{cases} 0.3711 \\ -1.553 \ . \end{cases} \tag{42}$$

Substituting these values into Eqs. (39a) and (39b) gives

$$\Delta a_n / \Delta a_{n+1} = \frac{C_{11} + C_{12}}{r} = \begin{cases} 8.721 & \text{for } r = r_1 \ , \\ -15.07 & \text{for } r = r_2 \ ; \end{cases} \tag{43a}$$

$$\Delta b_n / \Delta b_{n+1} = \frac{C_{21} + C_{22}}{r} = \begin{cases} 8.721 & \text{for } r = r_1 \ , \\ -15.07 & \text{for } r = r_2 \ . \end{cases} \tag{43b}$$

That is, along the lines described by Eq. (36) with the value of r given by Eq. (42), the eigenvalues of the renormalization-group operator are δ_1 and δ_2 respectively.

E. Coordinate transformation in search of the orbital scaling

To study the orbital scaling, let us recall that there are two scaling factors in 2D area-preserving maps, i.e., one along and one across the dominant symmetry line. A reasonable generalization to 4D maps is then that there are two sets of scaling factors: One set along, and the other across the dominant symmetry surface.

In general, the dominant symmetry surface of a 4D symplectic map has a curvature different from zero. It is obvious that it will be more convenient to study the orbital scaling if the dominant symmetry surface is a plane. A coordinate transformation for the 4D Hénon-like map

$$\begin{bmatrix} X \\ Y \end{bmatrix} \rightarrow \begin{bmatrix} U \\ V \end{bmatrix} = \begin{bmatrix} X \\ -Y + \frac{1}{2} F(X) \end{bmatrix} \tag{44}$$

converts the dominant symmetry surface (23) to a plane $V = 0$.

In the following, we will still use for convenience the notation $(X, Y) = (x, z, y, t)$, instead of (U, V), to express the new coordinates. In this notation the dominant symmetry plane is

$$Y = \begin{bmatrix} y \\ t \end{bmatrix} = 0 \ . \tag{45}$$

F. Scaling factors along the dominant symmetry surface

Using the scaling-matrix method, we define a 2×2 scaling matrix $\tilde{\alpha}_n$ on the dominant symmetry plane for a period-2^n orbit

$$\begin{bmatrix} x_0^{(n-1)} & -x_{2^n-2}^{(n-1)} \\ z_0^{(n-1)} & z_{2^n-2}^{(n-1)} \end{bmatrix} = \tilde{\alpha}_n \begin{bmatrix} x_0^{(n)} & -x_{2^n-1}^{(n)} \\ z_0^{(n)} & z_{2^n-1}^{(n)} \end{bmatrix} \ . \tag{46}$$

Using the data in Table II, we find that $\tilde{\alpha}_n$ converges quite well as n tends to infinity.

$$\tilde{\alpha}_n \rightarrow \tilde{\alpha} = \begin{bmatrix} \alpha_{11} & \alpha_{12} \\ \alpha_{21} & \alpha_{22} \end{bmatrix} = \begin{bmatrix} -3.840 & 7.940 \\ 0.4476 & 15.96 \end{bmatrix} \text{ as } n \rightarrow \infty \ . \tag{47}$$

One eigenvalue (α_1, say) of the scaling matrix $\tilde{\alpha}$ is found to be the same as the orbital scaling factor along the symmetry line in 2D area-preserving maps, and the other eigenvalue is its square,

$$\alpha_1 = -4.018\,076\,704 \ , \tag{48a}$$

$$\alpha_2 = 16.1449 = \alpha_1^2 \ . \tag{48b}$$

G. Orbital scaling factors across the dominant symmetry surface

Similar to what has been done for the orbital scaling factor along the symmetry surface, we define an orbital scaling matrix $\tilde{\beta}_n$ on the plane perpendicular to the symmetry surface for the orbit of period 2^n,

$$\begin{bmatrix} y_{2^n-3}^{(n-1)} \\ t_{2^n-3}^{(n-1)} \end{bmatrix} = \tilde{\beta}_n \begin{bmatrix} y_{2^n-2}^{(n)} \\ t_{2^n-2}^{(n)} \end{bmatrix} \ . \tag{49}$$

A numerical calculation shows that β_n converges quite well to

$$\tilde{\beta}_n \rightarrow \tilde{\beta} = \begin{bmatrix} \beta_{11} & \beta_{12} \\ \beta_{21} & \beta_{22} \end{bmatrix} = \begin{bmatrix} 13.94 & -6.082 \\ -8.537 & -5.120 \end{bmatrix} \text{ as } n \rightarrow \infty \tag{50}$$

One eigenvalue of the scaling matrix $\tilde{\beta}$ is the same as the orbital scaling factor across the symmetry line in 2D area-preserving maps, and the other is, within numerical accuracy, half of δ_2 (see Table III).

$$\beta_1 = 16.36 \ , \tag{51a}$$

$$\beta_2 = -7.5393 = \frac{\delta_2}{2} \ . \tag{51b}$$

We have also tested other Hénon-like symplectic maps (17) with

$$h(u) = \begin{cases} u^4 \\ \sin u^2 \ , \end{cases} \tag{52}$$

and obtained the same δ's, α's, and β's as that for the quadratic function. Therefore, universality seems to be well obeyed.

V. SUMMARY

We have succeeded in finding a complete period-doubling sequence in 4D symplectic maps. There exist two universal bifurcation rates δ_1 and δ_2, which imply that the fixed-point function has two relevant eigenvalues under the renormalization transformation. Within numerical precision, we also found $\delta_2=2\alpha_1\beta_1/\delta_1$, $\alpha_2=\alpha_1^2$, and $\beta_2=\frac{1}{2}\delta_2$. The relation $\alpha_2=\alpha_1^2$ is similar to the two-dimensional cases where α^2 rescaling emerges due to the curvature of the symmetry line. However, we have no clue as to why $\delta_2=2\alpha_1\beta_1/\delta_1$ and $\beta_2=\frac{1}{2}\delta_2$. Since there exist such relations among the exponents, there looms the possibility that the four-dimensional symplectic map we studied here is a degenerate case of two-dimensional maps.

It would be very desirable to understand the universality of period-doubling in four-dimensional symplectic maps by studying functional renormalization-group equations. This study would shed more light on such new features as the existence of a new unstable direction, the commonality of exponents between two and four dimensions, and the relations among the exponents.

ACKNOWLEDGMENTS

Two of us (J.M.M. and I.S.) would like to thank R.S. Mackay, R. Helleman, and K. Kaneko for their comments and useful discussions. One of us (J.M.) is grateful to Center for Nonlinear Studies (CNLS) at Los Alamos and Center for Studies of Nonlinear Dynamics (CSND) at La Jolla for their hospitality. This work was supported in part by the U.S. Department of Energy under Contract No. DE-AC02-84ER40182 and the University of Houston Advanced Research Program. The center for Studies of Nonlinear Dynamics is affiliated with the University of California, San Diego.

---

*Permanent address: Bartol Research Foundation, University of Delaware, Newark, DE 19711.

[1]J. M. Greene, R. S. Mackay, F. Vivaldi, and M. J. Feigenbaum, Physica **3D**, 468 (1981).

[2]T. C. Bountis, Physica **3D**, 577 (1981).

[3]T. Bountis and R. H. G. Helleman, J. Math. Phys. **22**, 1867 (1981).

[4]P. Collet, J.-P. Eckmann, and H. Koch, Phyisca **3D**, 457 (1981).

[5]R. Broucke, American Institute of Aeronautics & Astronautics J. **7**, 6 (1969).

[6]R. S. MacKay, Ph.D. dissertation, Princeton University, 1982.

[7]I. Satija and B. Hu (unpublished).

[8]T. Janssen and J. A. Tjon, J. Phys. A **16**, 673 (1983); **16**, 697 (1983).

[9]J. M. Mao, I. Satija, and B. Hu, Phys. Rev. A **32**, 1927 (1985).

[10]R. DeVogelaere, Technical Report 62-2, Department of Mathematics, University of California, Berkeley, 1962 (unpublished); *Theory of Nonlinear Oscillations,* edited by S. Lefschetz (1958), Vol. IV, p. 53.

[11]J. Guckenheimer, B. Hu, and J. Rudnick (unpublished).